

# Entangled self-phase locked states of light

H. H. Adamyan<sup>1,2,\*</sup> and G. Yu. Kryuchkyan<sup>1,2,†</sup>

<sup>1</sup>*Yerevan State University, A. Manoosyan 1, 375049, Yerevan, Armenia*

<sup>2</sup>*Institute for Physical Research, National Academy of Sciences,  
Ashtarak-2, 378410, Armenia*

We explore in detail the possibility of generation of continuous-variable (CV) entangled states of light fields with well-localized phases. We show that such quantum states, called entangled self-phase locked states, can be generated in nondegenerate optical parametric oscillator (NOPO) based on a type-II phase-matched down-conversion combined with polarization mixer in a cavity. A quantum theory of this device, recently realized in the experiment, is developed for both sub-threshold and above-threshold operational regimes. We show that the system providing relative phase coherence between two generated modes also exhibits different types of quantum correlations between photon numbers and phases of these modes. We quantify the entanglement as two-mode squeezing and show that CV entanglement is realized for both unitary, non-dissipative dynamics and for dissipative NOPO in the entire range of pump field intensities.

PACS numbers: 03.67.Mn, 42.50.Dv, 42.50.-p

## INTRODUCTION

It is now believed that entanglement of quantum composite systems with continuous degree of freedom is the basis of most applications in the field of Quantum Information [1]. Interest in continuous variable (CV) entanglement is being extensively excited by successful experiments on quantum teleportation based on two-mode squeezed states [2] as well as the experiments dealing with entanglement in atomic ensembles [3]. Since then, remarkable theoretical and experimental efforts have been devoted to generating and quantifying CV entangled states.

In this paper we propose a novel type of CV entangled states of light-field, which contain well-localized phases. They are different from the well-known entangled Einstein-Podolsky-Rosen (EPR) states generated in a nondegenerate optical amplifier [4, 5], which exhibit large phase fluctuations. We believe that such entangled states can be generated in a self-phase locked nondegenerate optical parametric oscillator (NOPO), based on the type-II phase-matched down-conversion and additional phase localizing mechanisms stipulated by the intracavity waveplate. The motivations for this study are the following:

For the first time the CV entangled states of light were studied in [4] and demonstrated experimentally in [5] for nondegenerate optical parametric amplifier (NOPA). Then a CV entanglement source was built from two single-mode squeezed vacuum states combined on a beamsplitter [2]. It is well known that each of the orthogonally polarized and frequency degenerate fields generated by NOPO is a field of zero-mean values. The phase sum of generated modes is fixed by the phase of the pump laser, while their phase difference undergoes a phase diffusion process [4] stipulated by vacuum fluctuations. As a rule, the NOPO phase diffusion noise is

substantially greater than the shot noise level, that limits the usage of NOPO in precision phase-sensitive measurements. Various methods based on phase locking mechanisms [6, 7, 8, 9, 10] have been proposed for reducing such phase diffusion. In the comparatively simple scheme realized in the experiment [6], self-phase locking was achieved in NOPO by adding an intracavity quarter-wave plate to provide polarization mixing between polarized signal and idler fields. The evidence of self-phase locking was provided there by the high level of phase coherence between the signal and idler fields. Following this experiment, the semiclassical theory of such NOPO was developed in [7]. Recently, the schemes of multiphoton parametric oscillators based on cascaded down-conversion processes in  $\chi^{(2)}$  media placed inside the same cavity and showing self-phase locking have been proposed [8]. As was demonstrated in [9], the system based on combination of OPO and second harmonic generation also displays self-phase locking. The formation of self-phase locking and its connection with squeezing in the parametric four-wave mixing under two laser fields has been demonstrated in [10]. An important characteristic of self-phase locked devices concerns the phase structure of generated subharmonics. Indeed, the formation of the variety of distinct phase states under self-phase locked conditions has been obtained in the mentioned Refs. [6, 7, 8, 9, 10]. It was recently noted that the schemes involving phase locking are potentially useful for precise interferometric measurements and optical frequency division because they combine fine tuning capability and stability of type - II phase matching with effective suppression of phase noise. That is why we believe it will be interesting to consider phase locked dynamics also from the perspective of Quantum Optics and, in particular, from the standpoint of production of CV entanglement.

A further motivation for such task is connected with the problem of experimental generation of bright entan-

gled light. So far, to the best of our knowledge, there is no experimental demonstration of CV entanglement above the threshold of NOPO. The progress in experimental study of bright two-mode entangled state from cw nondegenerate optical parametric amplifier has been made in [11]. The theoretical investigation of CV entangled light in transition through the generation threshold of NOPO is given in [12]. One of the principal experimental difficulties in advance toward a high-intensity level is the impossibility to control the frequency degeneration of modes above the threshold. We hope that the usage of phase locked NOPO may open a new interesting possibility to avoid this difficulty.

In this paper we report what is believed to be the first investigation of self-phase locked CV entangled states. We develop the quantum theory of self-phase locked NOPO, with decoherence included, in application to the generation of such entangled states. This scheme is based on the combination of two processes, namely, type-II parametric down-conversion and linear polarization mixer with cavity-induced feedback. The parametric down-conversion is a standard technique used to produce an entangled photon pairs as well as CV two-mode squeezed states [2]. The beam splitter including polarization mixer are also considered as experimentally accessible devices for production of entangled light-fields [13]. Besides these, there have been some studies of a beam splitter for various nonclassical input states, including two-mode squeezing states [14]. It is obvious, and also follows from the results of the mentioned papers [8, 9, 10], that the operational regimes of the combined system with cavity-induced feedback and dissipation drastically differ from those for pure processes. We show below that analogous situation takes place in the investigation of quantum-statistical properties of a combined system such as the self-phase locked NOPO.

The paper is arranged as follows. In Section II we formulate the model of combined NOPO based on the processes of two-photon splitting and polarization mixing, and present a semiclassical analysis of the system. Section III is devoted to the analysis of quantum fluctuations of both modes within the framework of linearization procedure around the stable steady-state. In Section IV we investigate the CV entangling resources of self-phase locked NOPO on the base of two-mode squeezing for both sub-threshold and above-threshold operational regimes. We summarize our results in Section V.

## MODEL OF SELF-PHASE LOCKED NOPO

As an entangler we consider the combination of two processes in a triply resonant cavity, namely, the type - II parametric down-conversion in  $\chi^{(2)}$ - medium and polarization mixing between subharmonics in lossless symmetric quarter-wave plate. The Hamiltonian describing

intracavity interactions is

$$\begin{aligned}
 H = & i\hbar E \left( e^{i(\Phi_L - \omega t)} a_3^\dagger - e^{-i(\Phi_L - \omega t)} a_3 \right) \\
 & + i\hbar k \left( e^{i\Phi_k} a_3 a_1^\dagger a_2^\dagger - e^{-i\Phi_k} a_3^\dagger a_1 a_2 \right) \\
 & + \hbar\chi \left( e^{i\Phi_\chi} a_1^\dagger a_2 + e^{-i\Phi_\chi} a_1 a_2^\dagger \right), \quad (1)
 \end{aligned}$$

where  $a_i$  are the boson operators for the cavity modes  $\omega_i$ . The mode  $a_3$  at frequency  $\omega$  is driven by an external field with amplitude  $E$  and phase  $\Phi_L$ , while  $a_1$  and  $a_2$  describe subharmonics of two orthogonal polarizations at degenerate frequencies  $\omega/2$ . The constant  $k e^{i\Phi_k}$  determines the efficiency of the down-conversion process. Linear coupling constant denoted as  $\chi e^{i\Phi_\chi}$  describes the energy exchange between the modes and besides,  $\chi$  is determined by the amount of polarization rotation due to the intracavity waveplate,  $\Phi_\chi$  determines the phase difference between the transformed modes. We take into account the detunings of subharmonics  $\Delta_i$  and the cavity damping rates  $\gamma_i$  and consider the case of high cavity losses for pump mode ( $\gamma_3 \gg \gamma$ ). However, in our analysis we take into account the pump depletion effects. The reduced density operator  $\rho$  within the framework of the rotating wave approximation and in the interaction picture is governed by the master equation

$$\begin{aligned}
 \frac{\partial \rho}{\partial t} = & \frac{1}{i\hbar} [H_{int}, \rho] + \sum_{i=1,2} \gamma_i (2a_i \rho a_i^\dagger - a_i^\dagger a_i \rho - \rho a_i^\dagger a_i) \\
 & + \frac{k^2}{\gamma_3} (2a_1 a_2 \rho a_1^\dagger a_2^\dagger - a_1^\dagger a_1 a_2^\dagger a_2 \rho - \rho a_1^\dagger a_1 a_2^\dagger a_2), \quad (2)
 \end{aligned}$$

where

$$\begin{aligned}
 H_{int} = & \hbar \Delta_1 a_1^\dagger a_1 + \hbar \Delta_2 a_2^\dagger a_2 \\
 & + i\hbar \frac{kE}{\gamma_3} (a_1^\dagger a_2^\dagger - a_1 a_2) + \hbar\chi (a_1^\dagger a_2 + a_1 a_2^\dagger). \quad (3)
 \end{aligned}$$

Let us also note that this equation is rewritten through the transformed boson operators  $a_i \rightarrow a_i \exp(-i\Phi_i)$ , with  $\Phi_i$  being  $\Phi_3 = \Phi_L$ ,  $\Phi_2 = \frac{1}{2}(\Phi_L + \Phi_k - \Phi_\chi)$ ,  $\Phi_1 = \frac{1}{2}(\Phi_L + \Phi_k + \Phi_\chi)$ . That leads to cancellation of the phases on the intermediate stages of calculations. As a result, the Hamiltonian  $H_{int}$  depends only on real-valued coupling constants. The appearance of the last term in the master equation means that the influence of the adiabatically eliminated fundamental mode is reduced to an additional loss mechanism for the subharmonic modes.

In order to proceed further, we now consider the phase-space symmetry properties of the system. It is easy to check that the interaction Hamiltonian satisfies the commutation relation  $[H_{int}, U(\pi)] = 0$  with the operator  $U(\theta) = \exp[i\theta (a_1^\dagger a_1 - a_2^\dagger a_2)]$ . Moreover, analogous symmetry  $[\rho(t), U(\pi)] = 0$  takes place for the density operator of the system, which obeys the master equation (2). Using this symmetry we establish the following selection rules for the normal-ordered moments of the mode

operators:

$$\langle a_1^{+k} a_2^{+m} a_1^l a_2^n \rangle = 0, \quad (4)$$

if  $k + l + m + n \neq 2j$ ,  $j = 0, \pm 1, \pm 2, \dots$ . Another peculiarity of NOPO with Hamiltonian (1) is displayed in the phase space of each of the subharmonic modes. The reduced density operator for each of the modes is constructed from the density operator  $\rho$  by tracing over the other mode  $\rho_{1(2)} = \text{Tr}_{2(1)}(\rho)$ . Therefore, we find that  $[\rho_1(t), U_1(\pi)] = [\rho_2(t), U_2(\pi)] = 0$ , where  $U_i(\theta) = \exp(i\theta a_i^\pm a_i)$ , ( $i = 1, 2$ ) is the rotation operator. It is easy to check using these equations that the Wigner functions  $W_1$  and  $W_2$  of the modes have a two-fold symmetry under the rotation of the phase-space by angle  $\pi$  around its origin,

$$W_i(r, \theta) = W_i(r, \theta + \pi), \quad (5)$$

where  $r, \theta$  are the polar coordinates of the complex phase space. Note, that such symmetry relationships (4), (5) radically differ from those taking place for the usual NOPO without the quarter-wave plate. Indeed, in this case, (case of  $\chi = 0$  in Eqs. (1)-(3)) the Wigner functions  $W_i$  are rotationally symmetric and the symmetry properties (4) read as  $\langle a_1^{+k} a_1^l a_2^{+m} a_2^n \rangle = 0$ , if  $k - l \neq m - n$ .

We perform concrete calculations in the positive P-representation [15] in the frame of stochastic equations for the complex c-number variables  $\alpha_i$  and  $\beta_i$  corresponding to the operators  $a_i$  and  $a_i^\dagger$

$$\begin{aligned} \frac{\partial \alpha_1}{\partial t} &= -(\gamma_1 + i\Delta_1) \alpha_1 \\ &+ (\varepsilon - \lambda \alpha_1 \alpha_2) \beta_2 - i\chi \alpha_2 + R_1, \end{aligned} \quad (6)$$

$$\begin{aligned} \frac{\partial \beta_1}{\partial t} &= -(\gamma_1 - i\Delta_1) \beta_1 \\ &+ (\varepsilon - \lambda \beta_1 \beta_2) \alpha_2 + i\chi \beta_2 + R_1^\dagger. \end{aligned} \quad (7)$$

Here  $\varepsilon = kE/\gamma_3$ ,  $\lambda = k^2/\gamma_3$ . The equations for  $\alpha_2, \beta_2$  are obtained from (6), (7) by exchanging the subscripts (1) $\rightleftharpoons$ (2).  $R_{1,2}$  are Gaussian noise terms with zero means and the following nonzero correlators:

$$\langle R_1(t) R_2(t') \rangle = (\varepsilon - \lambda \alpha_1 \alpha_2) \delta(t - t'), \quad (8)$$

$$\langle R_1^\dagger(t) R_2^\dagger(t') \rangle = (\varepsilon - \lambda \beta_1 \beta_2) \delta(t - t'). \quad (9)$$

In this approach the stochastic amplitude  $\alpha_3$  is given by  $\alpha_3 = (E - k\alpha_1\alpha_2)/\gamma_3$ . So, Eqs.(6)-(9) involve the depletion effect of the pump mode, which leads to the appearance of the above-threshold operational regime.

First, we shall study the steady-state solution of the stochastic equations in semiclassical treatment, ignoring the noise terms for the mean photon numbers  $n_{j0}$  and

phases  $\varphi_{j0}$  of the modes ( $n_j = \alpha_j \beta_j$ ,  $\varphi_j = \frac{1}{2i} \ln(\alpha_j/\beta_j)$ ). The mean photon numbers read as

$$n_{10}^\pm = \frac{1}{\lambda} \left( \frac{\Delta_2}{\Delta_1} \right)^{1/2} \left[ \sqrt{\varepsilon^2 - (\varepsilon_{cr}^\pm)^2 + \tilde{\gamma}^2} - \tilde{\gamma} \right], \quad (10)$$

$$n_{20}^\pm = \frac{1}{\lambda} \left( \frac{\Delta_1}{\Delta_2} \right)^{1/2} \left[ \sqrt{\varepsilon^2 - (\varepsilon_{cr}^\pm)^2 + \tilde{\gamma}^2} - \tilde{\gamma} \right], \quad (11)$$

where

$$\tilde{\gamma} = \frac{\gamma_1}{2} \left( \frac{\Delta_2}{\Delta_1} \right)^{1/2} + \frac{\gamma_2}{2} \left( \frac{\Delta_1}{\Delta_2} \right)^{1/2}. \quad (12)$$

As we can see from (10), (11),  $n_{10}^\pm$  and  $n_{20}^\pm$  are real and positive for  $\varepsilon$  exceeding two critical points

$$\begin{aligned} (\varepsilon_{cr}^\pm)^2 &= \gamma_1 \gamma_2 + \Delta_1 \Delta_2 + \chi^2 \\ &\mp \sqrt{4\chi^2 \Delta_1 \Delta_2 - (\gamma_1 \Delta_2 - \gamma_2 \Delta_1)^2}, \end{aligned} \quad (13)$$

and, besides, the solutions  $n_{i0}^+$  and  $n_{i0}^-$ , ( $i=1,2$ ) correspond to two distinct values  $\varepsilon_{cr}^+$  and  $\varepsilon_{cr}^-$  accordingly. The steady-state values of the phases corresponding to each of the critical points  $\varepsilon_{cr}^-$ ,  $\varepsilon_{cr}^+$  are obtained as

$$\begin{aligned} \sin(\varphi_{20}^+ - \varphi_{10}^+) &= \sin(\varphi_{20}^- - \varphi_{10}^-) = \\ &= \frac{1}{2\chi} \left[ \gamma_1 \left( \frac{\Delta_2}{\Delta_1} \right)^{1/2} - \gamma_2 \left( \frac{\Delta_1}{\Delta_2} \right)^{1/2} \right], \end{aligned} \quad (14)$$

$$\cos(\varphi_{20}^\pm + \varphi_{10}^\pm) = \frac{1}{\varepsilon} \sqrt{\varepsilon^2 - (\varepsilon_{cr}^\pm)^2 + \tilde{\gamma}^2}. \quad (15)$$

It is easy to check that these solutions exist for both modes only if the following relation holds

$$4\chi^2 \Delta_1 \Delta_2 > (\gamma_1 \Delta_2 - \gamma_2 \Delta_1)^2. \quad (16)$$

Let us note that the steady-state solutions (14), (15) completely determine the absolute phases of the orthogonally polarized modes, which are hence self-locked, unlike the ordinary NOPO. These results are in accordance with the ones obtained in [6, 7], but for another configuration of NOPO. In the scheme proposed in [6] only the signal and idler modes are excited in the cavity, while the pump field is a travelling wave. Nevertheless, in the adiabatic regime considered here there is correspondence between both schemes. Indeed, it is not difficult to check that the results (10), (11) transform to the corresponding results of the mentioned scheme [7] by replacing the parameter  $\varepsilon$  with the corresponding pump field amplitude.

We now turn to the standard linear stability analysis of these solutions, assuming for simplicity, the perfect symmetry between the modes, provided that the cavity decay rates and the detunings do not depend on the polarization ( $\gamma_1 = \gamma_2 = \gamma$ ,  $\Delta_1 = \Delta_2 = \Delta$ ). The stability of the

system is governed by the matrices  $F$  and  $F_+$ ,  $F_-$  describing the dynamics of small deviations  $\delta\alpha_i$  and  $\delta\beta_i$  from the semiclassical steady-state solutions (see, Sec.III). We reach stability if the real parts of eigenvalues of these matrices are positive. This analysis displays an evident dependence on the sign of the detunings  $\Delta_1 = \Delta_2 = \Delta$ . For the positive detuning,  $\Delta > 0$ , only the steady-state solutions  $n_{10}^- = n_{20}^-$  and  $\varphi_{20}^- - \varphi_{10}^-$ ,  $\varphi_{20}^- + \varphi_{10}^-$  are stable, while for the case of negative detuning the stability holds for the solutions with the (+) superscript. As this analysis shows, for either sign of detuning, the threshold is reached at  $\varepsilon \geq \varepsilon_{th}$ , where

$$\varepsilon_{th} = \sqrt{(\chi - |\Delta|)^2 + \gamma^2}, \quad (17)$$

and the steady-state stable solution for mean photon numbers can be written in the general form as

$$n_0 = n_{10} = n_{20} = \frac{1}{\lambda} \left[ \sqrt{\varepsilon^2 - (\chi - |\Delta|)^2} - \gamma \right]. \quad (18)$$

The phases are found to be

$$\varphi_{10} = \varphi_{20} = -\frac{1}{2} \text{Arc sin} \frac{1}{\varepsilon} (\chi + |\Delta|) + \pi k, \quad (19)$$

for  $\Delta > 0$ . For the opposite sign of the detuning,  $\Delta < 0$ , as we noted, the mean photon numbers are given by the same Eq.(18), while the phases read as

$$\begin{aligned} \varphi_{10} &= \frac{1}{2} \text{Arc sin} \frac{1}{\varepsilon} (\chi + |\Delta|) + \pi \left( k + \frac{1}{2} \right), \\ \varphi_{20} &= \frac{1}{2} \text{Arc sin} \frac{1}{\varepsilon} (\chi + |\Delta|) + \pi \left( k - \frac{1}{2} \right), \end{aligned} \quad (20)$$

( $k = 0, 1, 2, \dots$ ). In the region  $\varepsilon \leq \varepsilon_{th}$  the stability condition is fulfilled only for the zero amplitude steady-state solution  $\alpha_1 = \alpha_2 = \beta_1 = \beta_2 = 0$ . So, the set of above-threshold stable solutions for both modes have two-fold symmetry in the phase-space which was indeed expected from symmetry arguments (5).

Let us now consider the output behavior of the system for the special scheme of generation, when the couplings of in- and out-fields occur at only one of the ring-cavity mirrors. Taking into account that only the fundamental mode is coherently driven by the external field with  $\langle \alpha_3^{in} \rangle = E/\gamma_3$ , while the subharmonic modes are initially in the vacuum state, we obtain for the mean photon numbers (in units of photon number per unit time)  $n_3^{in} = E^2/2\gamma_3$ ,  $n_i^{out} = 2\gamma_i n_{i0}$  ( $i = 1, 2$ ) and hence  $n_1^{out} = n_2^{out} = 2\gamma n_0$ . Accordingly, parametric oscillation can occur above the threshold pump power  $P_{th} = \hbar\omega^3 E_{th}^2/2\gamma_3$ , where the threshold value of the pump field is equal to  $E_{th} = \frac{\gamma_3}{k} \sqrt{(\chi - |\Delta|)^2 + \gamma^2}$ .

We are now in a position to study quantum effects in self-phase locked NOPO and will state the main results of the paper concerning CV entanglement.

## ANALYSIS OF QUANTUM FLUCTUATIONS

The aim of the present section is to study the quantum-statistical properties of self-phase locked NOPO in linear treatment of quantum fluctuations. Quantum analysis of the system using  $P$ - representation is standard. A detailed description of the method can be found in [15]. We assume that the quantum fluctuations are sufficiently small so that Eqs.(6), (7) can be linearized around the stable semiclassical steady state  $\alpha_i(t) = \alpha_i^0 + \delta\alpha_i(t)$ ,  $\beta_i(t) = \beta_i^0 + \delta\beta_i(t)$ . This is appropriate for analyzing the quantum-statistical effects, namely CV entanglement, for all operational regimes with the exception of the vicinity of threshold, where the level of quantum noise increases substantially. It should also be emphasized at this stage that in the above-threshold regime of self-phase locked NOPO the steady-state phases of each of the modes are well-defined in contrast to what happens in the case of ordinary NOPO, where phase diffusion takes place. According to this effect, the difference between the phases, as well as each of the phases, can not be defined in the above-threshold regime of generation of the ordinary NOPO. On the whole, the well founded linearization procedure can not be applied for this case. Nevertheless, the linearization procedure and analysis of quantum fluctuations for ordinary NOPO become possible due to the additional assumptions about temporal behavior of the difference between the phases of the generated modes [16].

We begin with consideration of below-threshold operational regime, for  $E < E_{th}$ , where the equations linearized around the zero-amplitude solution can be written in the following matrix form

$$\frac{\partial}{\partial t} \delta\alpha^\mu = -F_{\mu\nu} \delta\alpha^\nu + R^\mu(\alpha, t), \quad (21)$$

where  $\mu = 1, 2, 3, 4$  and  $\delta\alpha^\mu = (\delta\alpha_1, \delta\alpha_2, \delta\alpha_3, \delta\alpha_4) = (\delta\alpha_1, \delta\alpha_2, \delta\beta_1, \delta\beta_2)$ ,  $R^\mu = (R_1, R_2, R_1^+, R_2^+)$ . The  $4 \times 4$  matrix  $F_{\mu\nu}$  is written in the block form

$$F = \begin{pmatrix} A & B \\ B^* & A^* \end{pmatrix} \quad (22)$$

with  $2 \times 2$  matrices

$$A = \begin{pmatrix} \gamma + i\delta & i\chi \\ i\chi & \gamma + i\delta \end{pmatrix}, \quad B = \varepsilon \begin{pmatrix} 0 & 1 \\ 1 & 0 \end{pmatrix}. \quad (23)$$

The noise correlators are determined as

$$\langle R^\mu(\alpha, t) R^\nu(\alpha, t') \rangle = D_{\mu\nu}(\alpha) \delta(t - t') \quad (24)$$

with the following diffusion matrix

$$D = \begin{pmatrix} B & 0 \\ 0 & B^* \end{pmatrix}. \quad (25)$$

First, we calculate the temporal correlation functions of the fluctuation operators. The expectation values of interest can be written as the integral

$$\langle \delta\alpha^\mu(t) \delta\alpha^\nu(t') \rangle = \int_{-\infty}^{\min(t,t')} d\tau \left( e^{F(t-\tau)} D e^{F^T(t'-\tau)} \right)_{\mu\nu}, \quad (26)$$

$F^T$  being the transposition of the matrix  $F$ . The integration over  $d\tau$  can be performed using the following useful formula for operators  $D F^T = F D$ , obtained by straightforward calculation. As a consequence, we arrive at the expression  $D e^{F^T t} = e^{F t} D$ . Finally we obtain

$$\langle \delta\alpha^\mu(t) \delta\alpha^\nu(t') \rangle = -\frac{1}{2} \left( F^{-1} e^{F|t-t'|} D \right)_{\mu\nu}, \quad (27)$$

and hence for  $t = t'$

$$\langle \delta\alpha^\mu(t) \delta\alpha^\nu(t) \rangle = -\frac{1}{2} (F^{-1} D)_{\mu\nu}. \quad (28)$$

This formula, however, is not very convenient for practical calculations. Therefore, we rewrite the correlation functions of the quantum fluctuations  $\delta\alpha_i, \delta\beta_i$  in a more simple form through the two-dimensional column vectors  $\delta\alpha = (\delta\alpha_1, \delta\alpha_2)^T, \delta\beta = (\delta\beta_1, \delta\beta_2)^T$ . Upon performing the calculation, we finally arrive at

$$\begin{aligned} \langle \delta\alpha (\delta\alpha)^T \rangle &= \frac{\varepsilon}{S^4 - 4\Delta^2\chi^2} \left[ \gamma \begin{pmatrix} -2\chi\Delta, & S^2 \\ S^2, & -2\chi\Delta \end{pmatrix} - i \begin{pmatrix} \chi(S^2 - 2\Delta^2), & \Delta(S^2 - 2\chi^2) \\ \Delta(S^2 - 2\chi^2), & \chi(S^2 - 2\Delta^2) \end{pmatrix} \right], \\ \langle \delta\alpha (\delta\beta)^T \rangle &= \frac{\varepsilon^2}{2(S^4 - 4\Delta^2\chi^2)} \begin{pmatrix} S^2, & -2\chi\Delta \\ -2\chi\Delta, & S^2 \end{pmatrix}, \end{aligned} \quad (29)$$

where  $S^2$  is introduced as

$$S^2 = \gamma^2 + \chi^2 + \Delta^2 - \varepsilon^2. \quad (30)$$

Note, that  $S^2 > 0$  in the below-threshold regime.

As an application of these results the mean photon number in the below-threshold regime can be calculated as follows,

$$n_1 = n_2 = \frac{\varepsilon^2 S^2}{2(S^4 - 4\Delta^2\chi^2)}. \quad (31)$$

Next we focus on the mode locked regime, for  $E > E_{th}$ , considering the Eqs. (6), (7) in terms of the fluctuations  $\delta n_i(t) = n_i(t) - n_{i0}$  and  $\delta\varphi_i(t) = \varphi_i(t) - \varphi_{i0}$  of photon number and phase variables. In this regime the dynamics described by the linearized equations of motion actually decouples into two independent dynamics for two groups of combinations  $\delta n_\pm = \delta n_2 \pm \delta n_1, \delta\varphi_\pm = \delta\varphi_2 \pm \delta\varphi_1$ . In fact, one has

$$\frac{\partial}{\partial t} \begin{pmatrix} \delta n_+ \\ \delta\varphi_+ \end{pmatrix} = -F_+ \begin{pmatrix} \delta n_+ \\ \delta\varphi_+ \end{pmatrix} + \begin{pmatrix} R_{n_+} \\ R_{\varphi_+} \end{pmatrix}, \quad (32)$$

$$\frac{\partial}{\partial t} \begin{pmatrix} \delta n_- \\ \delta\varphi_- \end{pmatrix} = -F_- \begin{pmatrix} \delta n_- \\ \delta\varphi_- \end{pmatrix} + \begin{pmatrix} R_{n_-} \\ R_{\varphi_-} \end{pmatrix}. \quad (33)$$

The drift,  $F_\pm$ , and the diffusion matrices,  $\langle R_i(t) R_j(t') \rangle = D_{ij}^{(+)} \delta(t-t')$ , ( $i, j = n_+, \delta\varphi_+$ );  $\langle R_n(t) R_m(t') \rangle = D_{nm}^{(-)} \delta(t-t')$ , ( $n, m = n_-, \varphi_-$ ) are respectively

$$F_+ = \begin{pmatrix} 2\lambda n_0, & 4n_0\varepsilon \sin(\varphi_{20} + \varphi_{10}) \\ 0, & 2(\gamma + \lambda n_0) \end{pmatrix}, \quad (34)$$

$$F_- = \begin{pmatrix} 2\gamma, & 4n_0\chi \sin n/\Delta \\ \Delta/n_0, & 0 \end{pmatrix}, \quad (35)$$

$$D^{(+)} = \begin{pmatrix} 4n_0\gamma, & -2\varepsilon \sin(\varphi_{20} + \varphi_{10}) \\ -2\varepsilon \sin(\varphi_{20} + \varphi_{10}), & -\gamma/n_0 \end{pmatrix}. \quad (36)$$

Due to the decoupling between (+) and (-) combinations of the modes, we conclude that the following temporal correlation functions are equal to zero,  $\langle \delta\varphi_+(t) \delta\varphi_-(t') \rangle = \langle \delta n_+(t) \delta n_-(t') \rangle = \langle \delta n_\pm(t) \delta\varphi_\mp(t') \rangle = 0$ , and hence  $\langle (\delta\varphi_1)^2 \rangle = \langle (\delta\varphi_2)^2 \rangle$ ,  $\langle (\delta n_1)^2 \rangle = \langle (\delta n_2)^2 \rangle$ . The other correlation functions can be calculated in the same way as described above for the below-threshold regime. The temporal correlation functions are derived as

$$\left\langle \begin{pmatrix} \delta n_\pm(t) \\ \delta\varphi_\pm(t) \end{pmatrix} (\delta n_\pm(t'), \delta\varphi_\pm(t')) \right\rangle = -\frac{1}{2} F_\pm^{-1} e^{-F_\pm^{-1}|t-t'|} D_\pm, \quad (37)$$

and hence

$$\left\langle \begin{pmatrix} \delta n_\pm \\ \delta\varphi_\pm \end{pmatrix} (\delta n_\pm, \delta\varphi_\pm) \right\rangle = -\frac{1}{2} F_\pm^{-1} D_\pm. \quad (38)$$

Performing the concrete calculations for each of the cases  $\Delta > 0$  and  $\Delta < 0$ , we arrive at the following results

$$\left\langle \left( \begin{array}{c} \delta n_+ \\ \delta \varphi_+ \end{array} \right) \left( \delta n_+, \delta \varphi_+ \right) \right\rangle = \frac{1}{4\lambda n_0(\gamma + \lambda n_0)} \left( \begin{array}{cc} 4n_0 [\gamma(\gamma + \lambda n_0) + (\chi - |\Delta|)^2], & -\lambda n_0(\chi - |\Delta|) \text{sign}(\Delta) \\ -2\lambda n_0(\chi - |\Delta|) \text{sign}(\Delta), & -\lambda \gamma \end{array} \right), \quad (39)$$

$$\left\langle \left( \begin{array}{c} \delta n_- \\ \delta \varphi_- \end{array} \right) \left( \delta n_-, \delta \varphi_- \right) \right\rangle = \frac{1}{4|\Delta|\chi} \left( \begin{array}{cc} 4n_0\chi(\chi - |\Delta|), & 2\chi\gamma \text{sign}(\Delta) \\ 2\chi\gamma \text{sign}(\Delta), & \frac{1}{n_0}(\gamma^2 - |\Delta|(\chi - |\Delta|)) \end{array} \right). \quad (40)$$

We see that the considered system displays different types of quantum correlations in terms of the stochastic variables, namely, between photon-number sum and phase sum in the modes, as well as between photon-number difference and phase difference in the modes. These results radically differ from the ones taking place for usual NOPO, where the correlation between photon-number difference and phase sum in the modes is realized. The results obtained indicate the possibilities to produce entanglement with respect to the new types of quantum correlations.

### CV ENTANGLEMENT IN THE PRESENCE OF PHASE LOCKING

Let us now turn our attention to quantum statistical effects and the entanglement production for the case of perfect symmetry between the modes ( $\gamma_1 = \gamma_2 = \gamma$ ,  $\Delta_1 = \Delta_2 = \Delta$ ). We note that unlike the two-mode squeezed vacuum state, the state generated in the above-threshold regime of NOPO is non-Gaussian, i.e. its Wigner function is non-Gaussian [17]. Recently, it has been demonstrated [18], that some systems involving beam splitters also generate non-Gaussian states. The general consideration of this problem for self-phase locked NOPO seems to be very complicated. However, the mentioned results allow us to conclude that the state generated in self-phase locked NOPO is most probably non-Gaussian. So far, the inseparability problem for bipartite non-Gaussian state is far from being understood. On the theoretical side, the necessary and sufficient conditions for the separability of bipartite CV systems have been fully developed only for Gaussian states, which are completely characterized by their first and second moments. To characterize the CV entanglement we address to both the inseparability and strong EPR entanglement criteria [19] which could be quantified by analyzing the variances of the relevant distance  $V_- = V(X_1 - X_2)$  and the total momentum  $V_+ = V(Y_1 + Y_2)$  of the quadrature amplitudes of two modes  $X_k = \frac{1}{\sqrt{2}} [a_k^+ \exp(-i\theta_k) + a_k \exp(i\theta_k)]$ ,  $Y_k = \frac{i}{\sqrt{2}} [a_k^+ \exp(-i\theta_k) - a_k \exp(i\theta_k)]$ , ( $k = 1, 2$ ), where  $V(X) = \langle X^2 \rangle - \langle X \rangle^2$  is a denotation for the variance and  $\theta_k$  is the phase of local oscillator for the k-th mode. The two quadratures  $X_k$  and  $Y_k$  are non commuting observables. The inseparability criterion for the quantum state

of two optical modes reads as [19]

$$V = \frac{1}{2}(V_+ + V_-) < 1, \quad (41)$$

i.e. indicates that the sum of variances drops below the level of vacuum fluctuations. Since the states of the system considered are non-Gaussian, the criterion (41) is only sufficient for inseparability. The strong EPR entanglement criterion is quantified by the product of variances as  $V_+ V_- < \frac{1}{4}$ . We remind that the sufficient condition for inseparability (41) in terms of the product of variances reads as  $V_+ V_- < 1$ , i.e. is weaker than the strong EPR condition.

In order to obtain the general expressions for variances, we first write them in terms of the boson operators corresponding to the Hamiltonian (1). We perform the transformations  $a_i \rightarrow a_i \exp(i\Phi_i)$ , which restore the previous phase structure of the intracavity interaction. Using also the symmetry relationships (4) we find quite generally the variances at some arbitrary quadrature phase angles  $\theta_1, \theta_2$  as

$$V_{\pm} = V \pm R \cos(\Delta\theta), \quad (42)$$

where

$$V = \frac{1}{2}(V_+ + V_-) = 1 + 2n - 2|\langle a_1 a_2 \rangle| \cos(\Sigma\theta + \Phi_{\text{arg}}), \quad (43)$$

$$R = 2 \text{Re}(\langle a_1^2 \rangle e^{i\Sigma\theta}) - 2|\langle a_1^+ a_2 \rangle|, \quad (44)$$

$$\Delta\theta = \theta_2 - \theta_1 - \Phi_{\chi}, \quad \Sigma\theta = \theta_1 + \theta_2 + \Phi_l + \Phi_k, \quad (45)$$

and  $n = \langle a_1^+ a_1 \rangle = \langle a_2^+ a_2 \rangle$  is the mean photon number of the modes,  $\Phi_{\text{arg}} = \arg \langle a_1 a_2 \rangle$ . So, in accordance with the formula (42), the relative phase  $\Phi_{\chi}$  between the transformed modes gives the effect of the rotation of the quadrature amplitudes angle  $\theta_2 - \theta_1$ .

Obviously, the variances  $V_{\pm}$  and hence the level of CV entanglement depend on all parameters of the system including the phases. The minimal possible level of  $V$  is realized for an appropriate selection of the phases  $\theta_i$ , namely for  $\theta_1 + \theta_2 = -\arg \langle a_1 a_2 \rangle - \Phi_l - \Phi_k$ . Further, in most cases we assume that this phase relationship takes place, but do not introduce new denotations for  $V$  and  $V_{\pm}$  for the sake of simplicity. In this case, ( $\Sigma\theta = -\Phi_{\text{arg}}$ ), in

correspondence with the formula (42), the variances  $V_{\pm}$  depend only on the difference between phases  $\Delta\theta$  and we arrive at

$$V = 1 + 2(n - |\langle a_1 a_2 \rangle|), \quad (46)$$

$$R = 2 \operatorname{Re}(\langle a_1^2 \rangle e^{-i\Phi_{\text{arg}}} - 2 |\langle a_1^+ a_2 \rangle|). \quad (47)$$

For the NOPO without additional polarization mixing  $\langle a_1^+ a_2 \rangle = \langle a_1^2 \rangle = \langle a_2^2 \rangle = 0$  and hence the case of the symmetric variances  $V_+ = V_-$  is realized. The phase-locked NOPO generally has non symmetric uncertainty region. However, the variances  $V_+$  and  $V_-$  become equal for the special case of  $\theta_2 - \theta_1 - \Phi_{\chi} = \frac{\pi}{2}$ , when the inseparability condition reads as  $V < 1$ , ( $V = V_- = V_+$ ). We note, that the relative phase  $\Phi_{\chi}$  plays an important role in specification of the entanglement.

### Entanglement in the case of unitary time-evolution

So far, we have considered mainly steady-state regime of generation, including the effects of dissipation and cavity-induced feedback. However, in order to better understand the peculiarities of the entanglement for the system under consideration, it would be interesting and desirable to study the case of a short interaction time  $t \ll \gamma^{-1}$ , when the dissipation in the cavity is unessential. In our analysis we shall assume that all processes are spontaneous, i.e. both subharmonic modes are initially in the vacuum state. Then, the system's state in the absence of losses is generated from the vacuum state by the unitary transformation

$$|\Psi(t)\rangle = u(t) |0\rangle_1 |0\rangle_2 = e^{-\frac{i}{\hbar} H_{int} t} |0\rangle_1 |0\rangle_2, \quad (48)$$

which for  $\chi \rightarrow 0$  gives two-mode squeezed vacuum state. Using formula (43), where  $n = \langle u^{-1}(t) a_i^+ a_i u(t) \rangle$  and  $\langle a_1(t) a_2(t) \rangle = \langle u^{-1}(t) a_1 a_2 u(t) \rangle$ , and also considering the case of zero-detunings  $\Delta_1 = \Delta_2 = \Delta = 0$ , after a long but straightforward algebra we get the final result for the variance  $V = \frac{1}{2}(V_+ + V_-)$  for two different operational regimes:  $\varepsilon < \chi$  and  $\varepsilon > \chi$ . The variance for the range  $\varepsilon < \chi$  of a comparatively weak scaled pump field  $\varepsilon = kE/\gamma_3$  reads as

$$V(t) = 1 - \frac{\varepsilon^2}{\mu^2} [\cos(2\mu t) - 1] - \frac{\varepsilon}{\mu} \sin(2\mu t) \cos(\Sigma\theta), \quad (49)$$

where  $\mu = \sqrt{\chi^2 - \varepsilon^2}$ . Thus, we observe a periodic evolution of  $V$  in this regime typical for the linear coupling. The level of squeezing of the two modes is periodically repeated. The behavior of the two-mode variance also significantly depends on the phase matching condition, so that we may tune the phase sum to maximize the

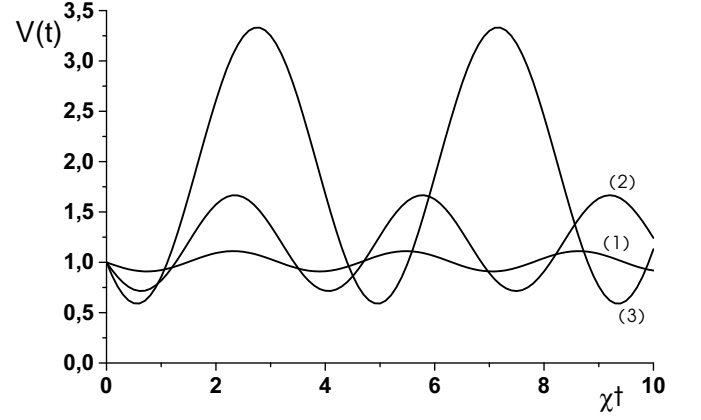


FIG. 1: Unitary evolution of the variance  $V(t)$  versus the scaled dimensionless interaction time  $\chi t$  for the range of  $\varepsilon < \chi$  and provided that  $\cos(\Sigma\theta) = 1$ . The parameters are:  $\varepsilon/\chi = 0.1$  (curve 1),  $\varepsilon/\chi = 0.4$  (curve 2) and  $\varepsilon/\chi = 0.7$  (curve 3).

entanglement. We further choose for illustrations the phase sum corresponding to  $\cos(\Sigma\theta) = 1$  for both operational regimes. The dependence of  $V$  versus the scaled time-interval is shown in Fig. 1, where the three curves correspond to three different choices of the ratio  $\varepsilon/\chi$ . Common to all curves is that the variance is nonclassical and squeezed at least at the points of its minima  $t_{\min}$ , which can be obtained by the formula  $ctg(2\mu t_{\min}) = \varepsilon/\mu$ . In all cases, the maximal degree of two-mode squeezing  $V_{\min} = V(t)|_{t=t_{\min}} = 0.5$  is achieved in the limit  $\varepsilon \rightarrow \chi$ . For the curves on the Fig. 1 the time-intervals corresponding to the minimal values of  $V_{\min}$  equal to  $\chi t_{\min} \simeq 0.74 + 1.005\pi k$  (curve 1),  $\chi t_{\min} \simeq 0.63 + 1.091\pi k$  (curve 2),  $\chi t_{\min} \simeq 0.57 + 1.4\pi k$  (curve 3), ( $k = 0, 1, 2, \dots$ ).

If the opposite inequality holds,  $\varepsilon > \chi$ , then the nonlinear parametric interaction becomes dominant over the linear coupling and the variance is given by the following formula

$$V(t) = 1 + \frac{\varepsilon^2}{\eta^2} [\cosh(2\eta t) - 1] - \frac{\varepsilon}{\eta} \sinh(2\eta t) \cos(\Sigma\theta), \quad (50)$$

where  $\eta = \sqrt{\varepsilon^2 - \chi^2}$ .

For  $\chi \rightarrow 0$  and  $\cos(\Sigma\theta) = 1$ , from this formula we arrive at a well-known result,  $V(t) = \exp(-2\varepsilon t)$ , for two-mode squeezed state. This shows that in the limit of infinite squeezing the corresponding state approaches to a simultaneous eigenstate of  $X_1 - X_2$  and  $Y_1 + Y_2$ , and thus becomes equivalent to the EPR state. Fig. 2 shows the behavior of  $V$  when the system operates in the regime  $\varepsilon > \chi$ . This figure clearly shows that as the interaction time increases, the variance decreases and reaches its minimum. Then the squeeze variance exponentially increases with the growth of the interaction time. For the data in Fig. 2 we obtain that the time intervals for which the variance reaches the minima are  $\chi t_{\min} \simeq 0.48$  (curve 1),

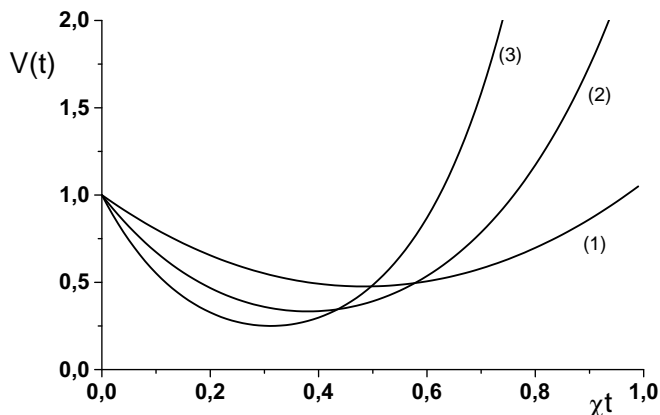


FIG. 2: Unitary time evolution of the variance  $V(t)$  for the range of  $\varepsilon > \chi$  and provided that  $\cos(\Sigma\theta) = 1$ . The parameters are:  $\varepsilon/\chi = 1.1$  (curve 1),  $\varepsilon/\chi = 2$  (curve 2) and  $\varepsilon/\chi = 3$  (curve 3).

$\chi t_{\min} \simeq 0.38$  (curve 2),  $\chi t_{\min} \simeq 0.31$  (curve 3). It is easy to check that these points of minima can be found by the formula  $ctgh(2\eta t_{\min}) = \varepsilon/\eta$ , provided that  $\cos(\Sigma\theta) = 1$ .

We also conclude that the variance squeezes up to a certain interaction time, if  $\varepsilon > \chi$ . It should be noted that although the time evolution of the variances are quite different for each of the operational regimes, the minimal values of the variance are described by the formula which is the same for both regimes

$$V_{\min} = V(t)|_{t=t_{\min}} = \frac{\chi}{\varepsilon + \chi}. \quad (51)$$

With increasing  $\varepsilon/\chi$ , in the regime  $\varepsilon > \chi$ , the minimal value of the variance decreases as  $V_{\min} \sim \chi/\varepsilon \ll 1$ , which means that perfect squeezing takes place in the limit of infinite pump field. This result is not at all trivial for the system considered, even in the absence of dissipation and cavity-induced feedback, because the insertion of polarization mixer usually destroys the two-mode squeezing produced by nondegenerate parametric down-conversion. The reason is that two-mode squeezed vacuum state is a superposition of two-photon Fock states  $|n\rangle_1 |n\rangle_2$  and the polarization mixer destroys the Fock states having the same number of photons, i.e.,  $n_1 = n_2 = n$ . The detailed analysis of this problem can be found, for example, in [14]

### Sub-threshold regime

Using formulas (29), (46), after some algebra, we obtain the minimal variance in the following form

$$V = 1 + \frac{\varepsilon \left( \varepsilon S^2 - \sqrt{\gamma^2 S^4 + \Delta^2 (S^2 - 2\chi^2)^2} \right)}{S^4 - 4\Delta^2 \chi^2}. \quad (52)$$

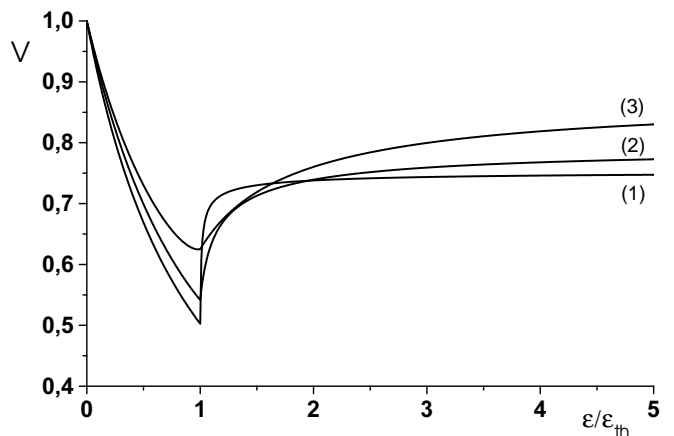


FIG. 3: Minimized variance  $V$  versus dimensionless amplitude of the pump field  $\varepsilon/\varepsilon_{th} = kE/\gamma_3 \sqrt{(\chi - |\Delta|)^2 + \gamma^2}$  for both operational regimes. The parameters are:  $\chi/\gamma = 0.1$ ,  $\Delta/\gamma = 10$  (curve 1),  $\chi/\gamma = 0.5$ ,  $\Delta/\gamma = 3$  (curve 2) and  $\chi/\gamma = 0.5$ ,  $\Delta/\gamma = 1$  (curve 3).

It is easy to check that in the limit  $\chi \rightarrow 0$  the variance coincides with the analogous one for the ordinary NOPO,  $V = V_- = V_+ = 1 - \varepsilon/(\varepsilon + \sqrt{\gamma^2 + \Delta^2})$ . We see that the minimal variance remains less than unity for all values of pump intensity and is a monotonically decreasing function of  $\varepsilon^2$ . For all parameters the maximal degree of two-mode squeezing  $V \simeq 0.5$  is achieved within the threshold range. It is also easy to check that this expression is well-defined for all values of  $\varepsilon^2$ , including the vicinity of the threshold. One should keep in mind, however, that the linear approach used does not describe the threshold range where the level of quantum fluctuations increases. As a consequence, some matrix elements of (29), (39), (40) increase infinitely in the vicinity of threshold. Nevertheless, it follows from (52) and further results (54)-(57), that such infinite terms are cancelled in the variance  $V$ , as well as in  $V_-$ ,  $V_+$  for both operational regimes. This is not surprising, since such cancellation of infinities in the quadrature amplitude variances takes place for the ordinary NOPO also.

One of the differences between the squeezing effects of the ordinary and self-phase locked NOPO is that the variances  $V_-$  and  $V_+$  for the ordinary NOPO are equal to each other, while for the self-phase locked NOPO they are in general different. The values of the non symmetric variances are expressed through  $R$  according to formula (42). This quantity can be calculated with the help of the formula (47). The result is found to be



$$R = \frac{\varepsilon\chi\Delta}{S^4 - 4\Delta^2\chi^2} \left[ \frac{\varepsilon^4 - (\gamma^2 + (\Delta - \chi)^2)(\gamma^2 + (\chi + \Delta)^2)}{\sqrt{\gamma^2 S^4 + \Delta^2(S^2 - 2\chi^2)^2}} + 2\varepsilon \right]. \quad (53)$$

As we see, the final expressions (52), (53) below the threshold are rather unwieldy. We show the corresponding numerical results on the Figs. 3, 4, 5 for illustration.

### Above-threshold regime

Performing calculations for each of the cases  $\Delta > 0$  and  $\Delta < 0$ , we find the variance  $V$  in the above-threshold regime in the following form

$$V = \frac{3}{4} - \frac{1}{4\sqrt{1 + (\varepsilon^2 - \varepsilon_{th}^2)/\gamma^2}} + \frac{\chi}{4|\Delta|}. \quad (54)$$

The results (52) and (54) for both operational regimes are summarized in Fig. 3, where the variance  $V$  is plotted as a function of the amplitude of the pump field. One can immediately grasp from the figure that the sum of variances  $V = \frac{1}{2}(V_+ + V_-)$  remains less than unity for all nonzero values of the pump field, provided that  $\chi < |\Delta|$ . This shows the nonseparability of the generated state. The maximal degree of entanglement is achieved in the vicinity of threshold,  $V \simeq 0,5$ , if  $\chi/|\Delta| \ll 1$ . In far above the threshold,  $E \gg E_{th}$ ,  $V$  increases with mean photon numbers of the modes and reaches the asymptotic value  $V = 3/4 + \chi/4|\Delta|$ . It should also be mentioned that the result (54) is expressed through the scaled pump field amplitude  $\varepsilon = kE/\gamma_3$  and hence depends on coupling constants  $k$  and  $\chi$ .

As the last step in connecting two-mode squeezing to observables of CV entanglement, we report the expressions of the non symmetric variances calculated with the help of the formulas (42), (46) and (47). Upon evaluating all required expectation values, we obtain

$$R = \frac{sgn(\Delta)}{4} \left( \frac{|\Delta| - \chi}{|\Delta|} - \frac{1}{\sqrt{1 + (\varepsilon^2 - \varepsilon_{th}^2)/\gamma^2}} \right) \quad (55)$$

and hence

$$V_+ = \frac{3|\Delta| + \chi + sgn(\Delta)\cos(\Delta\theta)(|\Delta| - \chi)}{4|\Delta|} - \frac{1 + sgn(\Delta)\cos(\Delta\theta)}{4\sqrt{1 + (\varepsilon^2 - \varepsilon_{th}^2)/\gamma^2}}, \quad (56)$$

$$V_- = \frac{3|\Delta| + \chi - sgn(\Delta)\cos(\Delta\theta)(|\Delta| - \chi)}{4|\Delta|} - \frac{1 - sgn(\Delta)\cos(\Delta\theta)}{4\sqrt{1 + (\varepsilon^2 - \varepsilon_{th}^2)/\gamma^2}}, \quad (57)$$

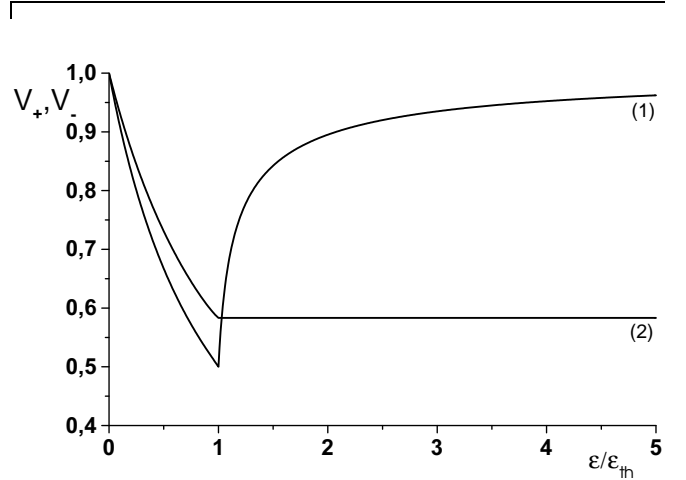


FIG. 4: The variances  $V_+$  (curve 1) and  $V_-$  (curve 2) versus the scaled pump field amplitude  $\varepsilon/\varepsilon_{th}$  for the parameters:  $\chi/\gamma = 0,5$ ,  $\Delta/\gamma = 3$ .

For the case of  $\Delta\theta = 0$ , when the variances are maximally different, the results are reduced to

$$V_- = \frac{1}{2} + \frac{\chi}{2\Delta}, \quad V_+ = 1 - \frac{1}{2\sqrt{1 + (\varepsilon^2 - \varepsilon_{th}^2)/\gamma^2}} \quad (58)$$

for  $\Delta < 0$ . The case of  $\Delta > 0$  is obtained from (58) by exchanging  $V_+ \rightarrow V_-$  and  $V_- \rightarrow V_+$ . These results for both operational regimes are depicted on Fig. 4. Some features are immediately evident. First of all one can see that both variances are minimal in the critical range but show quite different dependences on the ratio  $\varepsilon/\varepsilon_{th}$  above the threshold. Attentive reader may ask about dependence of the results obtained on parametric coupling constant  $k$ . We note in this connection that the squeezed variances are expressed through the scaled pump field amplitude  $\varepsilon = kE/\gamma_3$  and hence depend in general on both coupling constants  $k$  and  $\chi$ .

In terms of demonstrating the CV strong EPR entanglement, one has to apply another criterion  $V_+V_- < \frac{1}{4}$ . For the case of the symmetric uncertainties ( $V_+ = V_- = V$ ), the product of the variances  $V^2 \geq \frac{1}{4}$  and hence the strong EPR entanglement can not be realized. In the general case, the product of the variances reads as

$$V_+V_- = V^2 - R^2 \cos^2(\Delta\theta). \quad (59)$$

It seems that  $V_+V_-$  lies below  $1/4$  at least for the relative phase  $\Delta\theta = \pm\pi m$ , ( $m = 1, 2, \dots$ ), and in the vicinity of threshold, where  $V \simeq 0,5$ . However, for such selection of

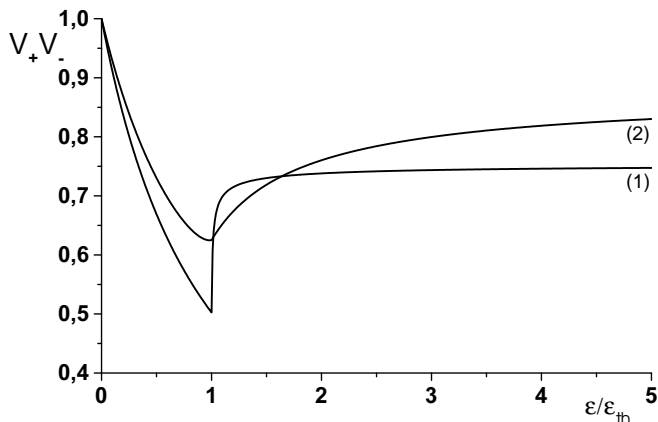


FIG. 5: The product of the variances  $V_+$  and  $V_-$  versus the scaled pump field amplitude  $\varepsilon/\varepsilon_{th}$  for the parameters  $\chi/\gamma = 0.1$ ,  $\Delta/\gamma = 10$  (curve 1) and  $\chi/\gamma = 0.5$ ,  $\Delta/\gamma = 1$  (curve 2).

the phases we arrive at

$$V_+ V_- = \frac{|\Delta| + \chi}{4|\Delta|} \left( 2 - \frac{1}{\sqrt{1 + (\varepsilon^2 - \varepsilon_{th}^2)/\gamma^2}} \right). \quad (60)$$

It is easy to check that the product of the variances exceeds  $\frac{1}{4}$  even in the vicinity of the threshold. This quantity for both operational regimes is illustrated in Fig. 5. It should be noted again that a detailed analysis of this problem, must include more accurate consideration of quantum fluctuations in the critical ranges.

## CONCLUSION

Our work demonstrates the possibility of creation of CV entangled light-states with well-localized phases. We show that such, so-called, entangled self-phase locked states of light can be generated in NOPO recently realized in the experiment [6]. This device is based on the type-II phase-matched down-conversion and additional phase localizing mechanisms stipulated by the intracavity waveplate. The novelty is that this device provides high level of phase coherence between the subharmonics in contrast to what happens in the case of ordinary NOPO, where the phase diffusion takes place. This development paves the way towards the generation of bright CV entangled light beams with well-localized phases. It looks like that this scheme involving phase locking may be potentially useful for precise interferometric measurements and quantum communications, because it combines quantum entanglement and stability of type - II phase matching with effective suppression of phase noise. The price one has to pay for these advantages is the small aggravation of the degree of CV entanglement in comparison with the case of ordinary NOPO. The quantum theory of self-phase locked NOPO has been developed in linear treatment of quantum fluctuations for both below- and

above-threshold regimes of generation. We have studied the CV entanglement as two-mode squeezing and have shown that entanglement is present in the entire range of pump intensities. In all cases the maximal degree of two-mode squeezing  $V \simeq 0,5$  is achieved in the vicinity of the threshold. It has also been shown that the amount of the entanglement can be controlled via the phase difference  $\Phi_\chi$ . The other peculiarities of the system of interest have been established for the case of unitary dynamics. One of these concerns the presence of two operational regimes generating two-mode squeezing. If the linear coupling between subharmonics dominates over the parametric down-conversion,  $\varepsilon < \chi$ , we have observed a periodic evolution of the squeezed variance. Maximal degree of squeezing has been  $V \simeq 0,5$  in this regime. If the parametric interaction becomes dominant,  $\varepsilon > \chi$ , the more high degree of two-mode squeezing can be obtained,  $V_{\min} = \frac{\chi}{\varepsilon + \chi} < 0,5$ , but up to certain interaction time.

In our analysis we have not investigated all possible quantum effects of self-phase locked parametric dynamics. In particular, we have noted that the system considered displays different types of quantum correlations, but we have not analyzed their connection with all possible kinds of the entanglement. Consideration of quantum fluctuations in the near threshold operational range of self-phase locked NOPO also deserves special attention for more accurate identification of CV entanglement. These topics are currently being explored and will be the subject of forthcoming work.

Acknowledgments: We thank J. Bergou for helpful discussions. This work was supported by the NFSAT PH 098-02 grant no. 12052 and ISTC grant no. A-823.

---

\* adam@unicad.am

† gkryuchk@server.physdep.r.am

- [1] Quantum Information Theory with Continuous Variables, S. L. Braunstein and A. K. Pati, eds. (Kluwer, Dordrecht, 2003), and references therein.
- [2] S. L. Braunstein and H. J. Kimble, Phys. Rev. Lett. **80**, 869 (1998); A. Furusawa, J. L. Sorensen, S. L. Braunstein, C. A. Fuchs, H. J. Kimble, and E. S. Polzik, Science **282**, 706 (1998); W. P. Bowen, N. Treps, R. Schnabel, and P. K. Lam, Phys. Rev. Lett. **89**, 253601 (2002).
- [3] J. Hald, J. L. Sorensen, C. Schori, and E. S. Polzik, Phys. Rev. Lett. **83**, 1319 (1999); B. Julsgaard, A. Kozhekin, and E. S. Polzik, Nature **413**, 400 (2000); A. Kuzmich, L. Mandel, and N. P. Bigelow, Phys. Rev. Lett. **85**, 1594 (2000); L. M. Duan, J. I. Cirac, P. Zoller, and E. S. Polzik, Phys. Rev. Lett. **85**, 5643 (2000).
- [4] M. D. Reid and P. D. Drummond, Phys. Rev. Lett. **60**, 2731 (1988); M. D. Reid, Phys. Rev. A **40**, 913 (1989); P. D. Drummond and M. D. Reid, Phys. Rev. A **41**, 3930, (1990).
- [5] Z. Y. Ou, S. F. Pereira, H. J. Kimble, and K. C. Peng, Phys. Rev. Lett. **68**, 3663 (1992); S. F. Pereira, Z. Y. Ou

- and H. J. Kimble, Phys. Rev. A **62**, 042311 (2002).
- [6] E. I. Mason, N. C. Wong, Opt. Lett. **23**, 1733 (1998).
- [7] C. Fabre, E. I. Mason, N. C. Wong, Opt. Comm. **170**, 299 (1999).
- [8] G. Yu. Kryuchkyan and N. T. Muradyan, Phys. Lett. A **286**, 113 (2001); G. Yu. Kryuchkyan, L. A. Manukyan and N. T. Muradyan, Opt. Comm. **190**, 245 (2001).
- [9] J. J. Zondy, A. Douillet, A. Tallet, E. Ressayre and M. L. Berre, Phys. Rev. Lett. A **63**, 023814 (2001).
- [10] G. Yu. Kryuchkyan, K. V. Kheruntsyan. Zh. Eksp. Teor. Fiz., **103**, 18 (1993); Zh. Eksp. Teor. Fiz., **104**, 1161 (1994).
- [11] Y. Zhang, H. Wang, X. Li, J. Jing, C. Xie, and K. Peng, Phys. Rev. A **62**, 023813 (2000); X. Li, Q. Pan, J. Jing, J. Zhang, C. Xie, K. Peng, Phys. Rev. Lett. **88**, 047904 (2002).
- [12] G. Yu. Kryuchkyan and L. A. Manukyan, quant-ph/0304205
- [13] B. C. Sanders, K. S. Lee and M. S. Kim, Phys. Rev. A **52**, 735 (1995); P. van Look and S. L. Braunstein, Phys. Rev. Lett. **84**, 3482 (2000).
- [14] M. S. Kim, W. Son, V. Buzek, and P. L. Knight, Phys. Rev. A **65**, 032323 (2002); WangXiang-bin, Phys. Rev. A **66**, 024303 (2002); *ibid.* A **66**, 064304 (2002).
- [15] P. D. Drummond, and C. W. Gardiner, J. Phys. A **13**, 2353 (1980); K. J. McNeil and C. W. Gardiner, Phys. Rev. A **28**, 1560 (1983).
- [16] M. D. Reid and P. D. Drummond, Phys. Rev. A **40**, 4493 (1989).
- [17] K. V. Kheruntsyan, K. G. Petrosyan, Phys. Rev. A **62**, 015801 (2000).
- [18] G. Toth, C. Simon, and J. I. Cirac, quant-ph/0306086.
- [19] L. M. Duan, G. Giedke, J. I. Cirac, and P. Zoller, Phys. Rev. Lett. **84**, 2722 (2000); R. Simon Phys. Rev. Lett. **84**, 2726 (2000); G. Giedke, B. Kraus, M. Lewenstein, and J. I. Cirac, Phys. Rev. Lett. **87**, 167904 (2001); R. F. Werner and M. M. Wolf, Phys. Rev. Lett. **86**, 3658 (2001).